

Composition and Material Properties of an MnO/H₂ Based Thermal Plasma

S. G. Johnsen¹ and S. Andersson¹

¹ Department of Metal Production and Processing, SINTEF, Trondheim, Norway

Abstract: Replacing carbon with hydrogen in the reduction of MnO to metallic manganese will require the development of novel plasma-based processes. Mathematical modelling of reactor operation will provide invaluable insight with respect to optimization and design choices. This paper reports computed temperature-dependent chemical equilibrium compositions and material properties for an MnO/H₂-based plasma.

Keywords: Manganese, hydrogen, plasma, chemical composition, material properties

1. Introduction

At SINTEF (dept. Metal production and processing, Trondheim, Norway), novel processes are developed to allow for carbon-free reduction of metal ores [1]. Using hydrogen (H₂) as reductant has been proposed as an attractive alternative to carbon (C), since the off-gas will consist of water vapour (H₂O) rather than carbon dioxide (CO₂). This has, e.g., been successfully demonstrated for iron ore reduction [2,3]. For other metal oxides, however, thermodynamic limitations prohibit reduction by diatomic hydrogen. It has been proposed to utilize hydrogen plasma rich in excited hydrogen molecules, monoatomic hydrogen (H) and hydrogen cations (H₂⁺ and H⁺), to promote thermodynamically favourable reduction reactions [4].

The proposed technology requires the development of novel plasma reactors, and mathematical modelling plays an important role in the design process. Due to extreme temperatures and tiny time- and length-scales, detailed measurements inside the reactor chamber are practically impossible. It is therefore required to establish computational fluid dynamics (CFD) models to assess decisions made during the design process. A crucial building block for the CFD models is the accurate representation of the plasma gas. In the current paper, we describe the development of a thermodynamic model, based on statistical mechanics and partition functions, for a system of manganese monoxide (MnO) and H₂. The model consists of complete lists of chemical species and their chemical reactions, material properties and energy spectra, and predictions of temperature- and pressure-dependent equilibrium chemical composition and enthalpies. Derived quantities include specific heat capacities at constant volume/pressure, adiabatic index, and speed-of-sound.

2. Method

In the following, a brief overview of the theoretical foundation for the current work is given. The methodology follows closely the classical textbooks by Boulos *et al.* [5] and Anderson [6], as well as the calculation framework by Reynolds *et al.* [7]. Derivation of the model relies on assumptions of thermodynamic equilibrium, equipartition of energy, and ideal mixtures of thermally perfect gasses, as well as standard methods from statistical physics.

The total partition function of an individual chemical species, i , is expressed as the product of the temperature-

dependent translational, rotational, vibrational, and electronic partition functions,

$$Q_i = Q_{tr,i} Q_{rot,i} Q_{vib,i} Q_{el,i} \quad (1)$$

In Table 1, an overview of the partition functions for various species types is given. The species-specific internal energy and sensible enthalpy are obtained from

$$e_i = \frac{RT^2}{M_i} \left(\frac{\partial \ln Q_i}{\partial T} \right)_V, \quad (2)$$

and

$$h_i = e_i + RT/M_i, \quad (3)$$

respectively, and the mixture's internal energy and enthalpy are defined by

$$e = \sum_{i=1}^{\mathcal{N}} x_i \left(e_i + (\Delta h_f)_i \right), \quad (4)$$

and

$$h = \sum_{i=1}^{\mathcal{N}} x_i \left(h_i + (\Delta h_f)_i \right). \quad (5)$$

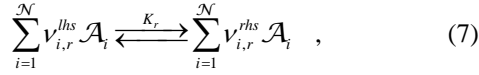
The specific heat capacities at constant volume and pressure are obtained by taking the numerical, partial derivatives of eqs. (4) and (5); $c_v = (\partial e / \partial T)_V$, and $c_p = (\partial h / \partial T)_P$. The speed of sound is obtained from [6];

$$c = \sqrt{\frac{\gamma RT}{M} \frac{1 + (1/P)(\partial e / \partial V)_T}{1 - \rho(\partial h / \partial P)_T}}. \quad (6)$$

Table 1. Overview of partition functions for species types included in the current study.

| Part. func. | Electron | Mono-atomic | Diatomic | Triatomic |
|-------------|----------|-------------|---|--|
| Q_{tr} | | | $\left(\frac{2\pi M k_B T}{N_A h^2} \right)^{3/2} V$ | |
| Q_{rot} | 1 | 1 | $\frac{k_B T}{\sigma_s B_e}$ | $\frac{\sqrt{\pi}}{\sigma_s} \left(\frac{k_B^3 T^3}{B_{e,1} B_{e,2} B_{e,3}} \right)^{1/2}$ |
| Q_{vib} | 1 | 1 | $\frac{1}{1 - \exp(-\omega_e / k_B T)}$ | $\prod_i \frac{1}{1 - \exp(-\omega_{e,i} / k_B T)}$ |
| Q_{el} | 2 | | $\sum_{m=0}^{\infty} g_m \exp(-\varepsilon_{el,m} / k_B T)$ | |

For a generic chemical equilibrium expressed as



the partial pressure-based equilibrium constant is given by

$$K_{P,r}(T) = (\Lambda k_B T)^{\sum_{i=1}^{\mathcal{N}} \Delta \nu_{i,r}} e^{-\Delta \epsilon_{0,r}/k_B T} \prod_{i=1}^{\mathcal{N}} \left(M_i^{\frac{3}{2}} Q_{int,i} \right)^{\Delta \nu_{i,r}}, \quad (8)$$

where $\Lambda \approx 5.943 \cdot 10^{-30} T^{3/2}$. The chemical equilibrium composition can be found by solving the set of equations given by

$$K_{P,r} = \prod_{i=1}^{\mathcal{N}} P_i^{\Delta \nu_{i,r}}, \quad (9)$$

in addition to conservation equations for the number of nuclei and the total electric charge.

3. Materials

In addition to electrons, 22 tri-/di-/monoatomic and ionic species based on hydrogen, oxygen, and manganese nuclei, were included in the present work. Rotational and vibrational excitations were limited to their ground states, but available electronic excitation data was utilized for all species. The complete list of modelled species and literature sources for their data are summarized in Table 2. The complete list of chemical reactions considered is given in Table 3.

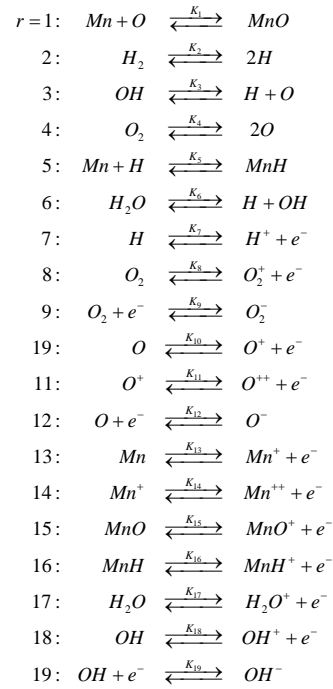
4. Results and Discussion

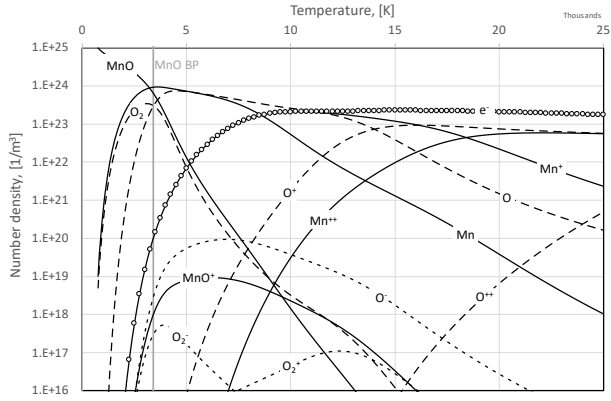
The temperature-dependent chemical equilibrium composition was computed for two feeds consisting of 1) 1 mole of pure MnO, and 2) 0.5 mol of MnO and 0.5 mol of H₂, at atmospheric pressure. The results are shown in figs. 1 and 2. The boiling point (BP) of MnO (3400 K) is indicated by vertical lines. It can be seen that dissociation of MnO, H₂, and O₂ takes place at temperatures close to the MnO boiling point, such that at higher temperatures, the monoatomic species are dominant. Mn⁺ ions are the dominant ionic species below 10 000 K. At higher temperatures, hydrogen and oxygen cations occur. Above 15 000 K, Mn⁺⁺ ions replace Mn⁺. The calculations indicate that MnO is practically non-existent at temperatures around and above 5000 K. Thus, the production of metallic Mn is feasible if the back reaction to MnO can be avoided during condensation/precipitation of liquid/solid Mn. This can be achieved by ensuring that O reacts with hydrogen, to form H₂O. In the absence of hydrogen (or some other reductant), however, the back reaction to MnO seems unavoidable. Further investigations, including experiments as well as chemical kinetics, phase-change, and mass/heat transport modelling, are needed to assess the likelihood of finding a novel, carbon-free process for Mn production based on hydrogen plasma. More detailed equilibrium

Table 2. List of modelled species and references to their required properties (ionization energy, formation enthalpy, rotational and vibrational constants, and electronic energy level data).

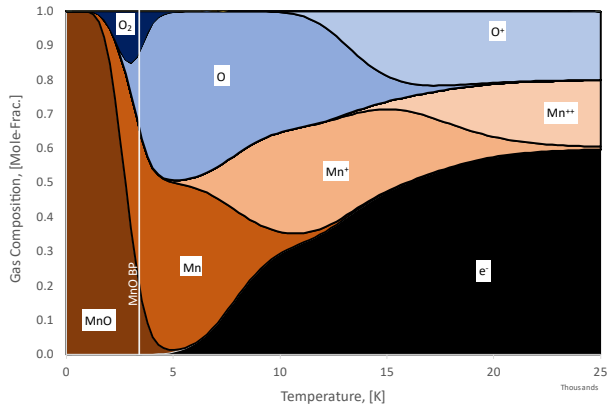
| | IE | Δh_f | B_e | ω_e | $g_m, \epsilon_{el,m}$ |
|-------------------------------|------|--------------|-------|------------|------------------------|
| e ⁻ | | | | | |
| MnO | [8] | [9] | [8] | [8] | [8] |
| H ₂ | [8] | | [8] | [8] | [8] |
| Mn | [8] | [8] | | | [10] |
| O | [8] | [8] | | | [10] |
| H | [8] | [8] | | | [10] |
| OH | [8] | [8] | [8] | [8] | [8] |
| O ₂ | [8] | | [8] | [8] | [8] |
| MnH | [8] | [9] | [8] | [8] | [8,11] |
| H ₂ O | [8] | [8] | [12] | [8] | [8] |
| H ⁺ | | | | | |
| O ₂ ⁺ | | | [8] | [8] | [8] |
| O ₂ ⁻ | [8] | [8] | [8] | [8] | [8,13] |
| O ⁺ | [10] | | | | [10] |
| O ⁺⁺ | | | | | [10] |
| O ⁻ | [8] | | | | [14] |
| Mn ⁺ | [10] | | | | [10] |
| Mn ⁺⁺ | | | | | [10] |
| MnO ⁺ | | | [15] | [15] | [8] |
| MnH ⁺ | | | [16] | [16] | [16] |
| H ₂ O ⁺ | | | [17] | [8] | [8] |
| OH ⁺ | | | [8] | [8] | [8] |
| OH ⁻ | [8] | | [8] | [8] | [18,19] |

Table 3. Overview of chemical reactions.

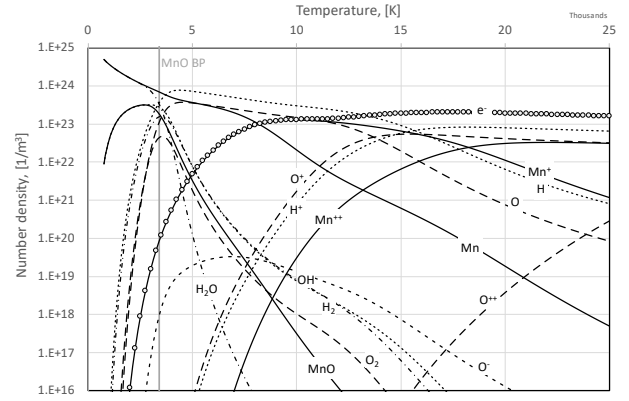




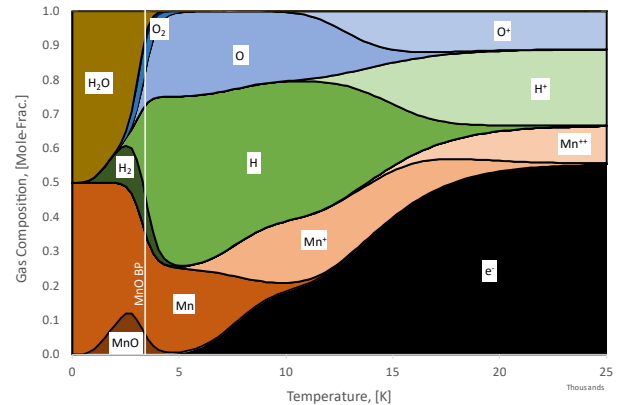
(a) Number densities of selected species.



(b) Mole-fractions.



(a) Number densities of selected species.



(b) Mole-fractions.

Fig. 1. Temperature dependent equilibrium composition based on a feed consisting of 1 mol MnO at 1 bara.

computations should also include additional anions (e.g. MnO^- and MnH^-) and triatomic species (e.g. MnOH , MnO_2 , MnH_2 , and MnH_2^+).

In Fig. 3, computed material properties (specific heat capacity, adiabatic index, and speed of sound) are shown for the MnO/H_2 feed, at selected pressures. The local maxima of the specific heat capacity are attributed to (counting from left to right): 1) the dissociation of MnO and H_2 ; 2) the ionization of Mn ; and 3) the ionization of H , O , and Mn^+ . Increasing the pressure shifts the local maxima towards higher temperatures and reduces their peak height.

5. Conclusions

A mathematical framework was established to compute chemical equilibrium compositions and material properties for MnO/H_2 based thermal plasmas. Preliminary results have been presented indicating that the use of plasma to generate monoatomic and ionic hydrogen species may be beneficial for the reduction of manganese ore. Further investigations are needed, including experiments as well as chemistry and transport modelling, to support the design of a novel plasma-based carbon-free process for the production of metallic manganese.

Fig. 2. Temperature dependent equilibrium composition based on a feed consisting of 0.5 mol of MnO and 0.5 mol of H_2 at 1 bara.

6. Acknowledgements

This work was funded by SINTEF, Trondheim, Norway.

7. Nomenclature

\mathcal{A}_i Symbol to denote species i .

c Speed of sound, $[m/s]$.

c_p Specific heat capacity at constant pressure, $[J/kgK]$.

c_v Specific heat capacity at constant volume, $[J/kgK]$.

e Specific internal energy, $[J/kg]$.

$\Delta\epsilon_0$ Heat of reaction, $[J/kg]$.

Δh_f Formation enthalpy, $[J/kg]$.

h Specific enthalpy, $[J/kg]$.

g_i Degeneracy (statistical weight) of energy level i .

$\gamma \equiv c_p/c_v$ Adiabatic index.

k_B Boltzmann constant, $[J/K]$.

$K_{p,r}$ Equilibrium constant of reaction r .

M Molar mass, $[kg/mol]$.

$v_{i,r}$ Stoichiometric coefficient of species i in reaction r .

\mathcal{N} Number of chemical species.

ω_e Vibrational constant, $[J]$.

P Pressure, $[Pa]$.

Q Partition function.

R Universal gas constant, $[J/molK]$.

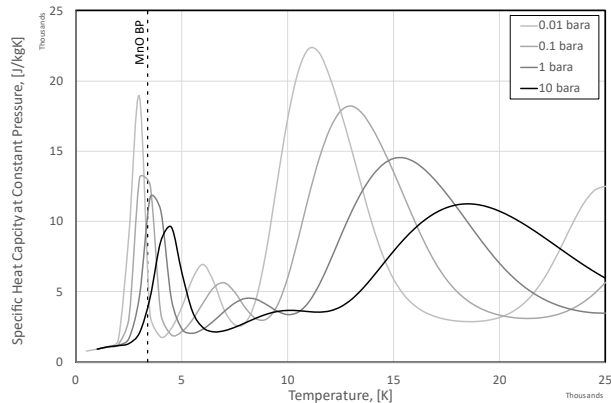
ρ Mass density, $[kg/m^3]$.

σ_s The symmetry constant.

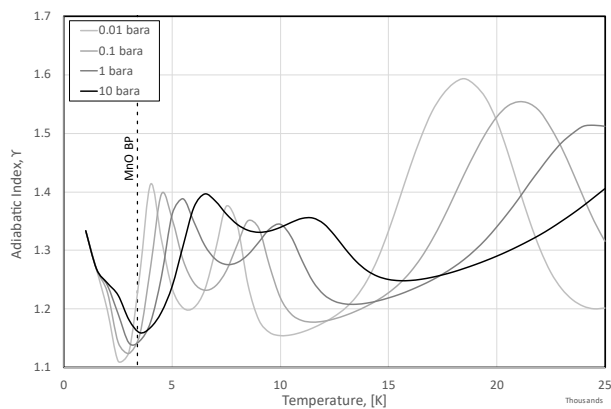
T Temperature, $[K]$.

V Volume, $[m^3]$.

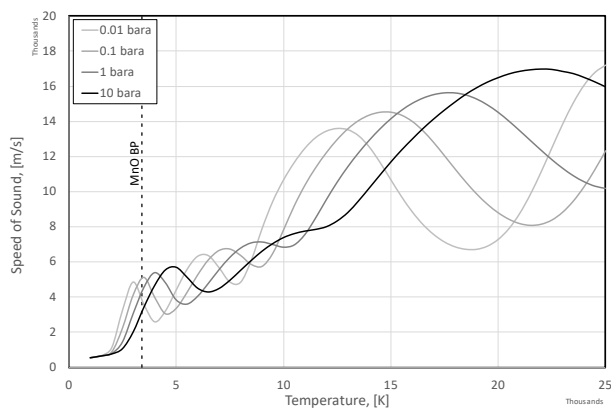
x_i Mass fraction of species i , $[kg/kg]$.



(a) Specific heat capacity.



(b) Adiabatic index.



(c) Speed of sound.

Fig. 3. Temperature dependent gas material properties, based on a feed consisting of 0.5 mol of MnO and 0.5 mol of H_2 .

8. References

- [1] H. Dalaker, <https://www.sintef.no/en/projects/2020/hypla-hydrogen-plasma-for-co2-free-metal-production/>.
- [2] D. Spreitzer and J. Schenk, *Steel Research Int.* **90**, 1900108 (2019).
- [3] F. Patisson and O. Mirgaux, *Metals* **10**, 922 (2020).
- [4] K. C. Sabat, P. Rajput, R. K. Paramguru, B. Bhoi, and B. K. Mishra, *Plasma Chem Plasma Process* **34**, 1 (2014).
- [5] M. I. Boulos, P. Fauchais, and E. Pfender, *Thermal Plasmas - Fundamentals and Applications*, Vol. 1 (Plenum Press, New York, 1994).
- [6] J. D. Anderson, *Hypersonic and High-Temperature Gas Dynamics*, 2nd ed (American Institute of Aeronautics and Astronautics, Reston, Va, 2006).
- [7] Q. Reynolds, M. Erwe, and C. Sandrock, <https://github.com/quinnreynolds/minplascalc>.
- [8] P. Linstrom and Mallard, W.G., editors, <https://doi.org/10.18434/T4D303>.
- [9] W. Jiang, N. J. DeYonker, J. J. Determan, and A. K. Wilson, *J. Phys. Chem. A* **116**, 870 (2012).
- [10] A. Kramida and Y. Ralchenko, <https://doi.org/10.18434/T4W30F>.
- [11] W. J. Balfour, *The Journal of Chemical Physics* **88**, 5242 (1988).
- [12] R. T. Hall and J. M. Dowling, *The Journal of Chemical Physics* **47**, 2454 (1967).
- [13] K. M. Ervin, I. Anusiewicz, P. Skurski, J. Simons, and W. C. Lineberger, *J. Phys. Chem. A* **107**, 8521 (2003).
- [14] H.-P. Popp, *Physics Reports* **16**, 169 (1975).
- [15] B. C. Sweeny, H. Pan, S. G. Ard, N. S. Shuman, A. A. Viggiano, N. Keyes, C. Xie, H. Guo, V. G. Ushakov, and J. Troe, *International Journal of Mass Spectrometry* **435**, 26 (2019).
- [16] D. J. D. Wilson, C. J. Marsden, and E. I. von Nagy-Felsobuki, *Phys. Chem. Chem. Phys.* **5**, 252 (2003).
- [17] R. Johnson, editor, <https://doi.org/10.18434/T47C7Z>.
- [18] N. H. Rosenbaum, J. C. Owrutsky, L. M. Tack, and R. J. Saykally, *The Journal of Chemical Physics* **84**, 5308 (1986).
- [19] B. S. D. R. Vamhindi and M. Nsangou, *Molecular Physics* **114**, 2204 (2016).